


# Determining the Eccentricity of Source Masses in the Measurement of Newtonian Gravitational Constant Using an Air-Bearing Method

Jian-Ping Liu<sup>1</sup>,<sup>\*</sup> Chao Xue,<sup>1,\*</sup> Bing-Peng Wang,<sup>2</sup> Qing Li,<sup>2</sup> Wen-Hai Tan,<sup>1</sup> Qi Liu,<sup>1</sup>  
Cheng-Gang Shao,<sup>2</sup> Liang-Cheng Tu,<sup>1</sup> Shan-qing Yang,<sup>1</sup> and Jun Luo<sup>1</sup>

<sup>1</sup>MOE Key Laboratory of TianQin Mission, TianQin Research Center for Gravitational Physics & School of Physics and Astronomy, Frontiers Science Center for TianQin, CNSA Research Center for Gravitational Waves, Sun Yat-sen University (Zhuhai Campus), Zhuhai 519082, China

<sup>2</sup>MOE Key Laboratory of Fundamental Physical Quantities Measurements & Huber Key Laboratory of Gravitation and Quantum Physics, PGMF and School of Physics, Huazhong University of Science and Technology, Wuhan 430074, China

 (Received 6 March 2023; revised 27 April 2023; accepted 7 June 2023; published 27 June 2023)

The metrological characteristics of source masses are essential in the determination of the Newtonian gravitational constant  $G$ . This paper presents an air-bearing method to check the density uniformity of spherical source masses by measuring the mass center offset from the geometric center. With detailed error analysis, we find that the eccentricity measurement accuracy using this method has the potential to be better than  $0.1\mu\text{m}$ , and the uncertainty of actual experimental measurement is mainly limited by the nonsphericity of spheres. Two kinds of spherical source masses that are directly used in measurements of  $G$  are measured. The eccentricity of the 57-mm-diameter spheres used in the time-of-swing method is determined to be less than  $0.3\mu\text{m}$  and that of the 127-mm-diameter spheres used in the angular acceleration feedback method is less than  $1.3\mu\text{m}$ . Two density distribution models are discussed to estimate the uncertainty in the value of  $G$  in terms of the density uniformity of source masses.

DOI: [10.1103/PhysRevApplied.19.064075](https://doi.org/10.1103/PhysRevApplied.19.064075)

## I. INTRODUCTION

The determination of the Newtonian gravitational constant  $G$  is a process of accurately quantifying the gravitational interaction between test mass and source mass. A precise  $G$  value greatly depends on a full knowledge of the metrological characteristics of the two masses [1], including shape, size, density homogeneity, magnetic performance, and so on. Extensive work has been done to eliminate or reduce the impact of these factors and this paper focuses on the problem of density homogeneity.

In the typical torsion pendulum scheme, the test masses are usually much smaller than the source masses as limited by the load of the suspension fiber with high sensitivity, and the influence of the density variation can be greatly reduced by a certain parameter design [2,3]. By contrast, the source masses usually have a larger density and size to produce as large a gravitational field as possible. The materials have included tungsten, stainless steel, lead, copper, copper alloy, and so on. And most of the experiments have employed masses in the shapes of spheres or cylinders [3–9]. It is more challenging to evaluate the density inhomogeneity of such large-scale metal objects.

The unreasonably large spread in the  $G$  values obtained by different groups [10] indicates that more efforts should be made to investigate the systematic errors in these experiments. Motivated by an intention to discover potential error sources and obtain a more reliable  $G$  value, our group carried out  $G$  measurements with two independent methods at the same period of time [11]: the time-of-swing (TOS) method and the angular acceleration feedback (AAF) method. In both types of  $G$  measurements, several SS316 stainless steel spheres are used as source masses (four 57-mm-diameter spheres are used in the TOS method and four 127-mm-diameter spheres are used in the AAF method). The spherical stainless source masses have the following advantages: high symmetry, convenient to calculate gravitational interaction, nonmagnetic material, and relatively easily processed to high precision. While the steel spheres are nontransparent and even high-energy rays do not easily pass through, it is difficult to measure the source masses' density distribution directly.

Previously a sphere from the same batch was cut into small blocks and scanned by an electron microscope. By the statistics of the scanning data we obtained the relative variation of the spheres' density to be about 0.06% over a volume of  $0.272 \times 0.234 \times 0.005 \text{ mm}^3$  [12]. Nevertheless, this method leads to damage of the spheres, and as a result

\*xuech7@mail.sysu.edu.cn

cannot be used to directly measure the spheres used in the experiments. And we can only obtain the local density distribution of a small piece of sample and the result is based on an assumption that other parts of the sphere follow the same distribution.

A supplementary method to check the density uniformity is measuring the mass center offset from the geometric center of the source masses. As a result, an air-bearing method, which is similar to the method used in JILA (Joint Institute for Laboratory Astrophysics, a joint institute of the University of Colorado Boulder and the National Institute of Standards and Technology, USA) [7] and BIPM (International Bureau of Weights and Measures, France) [8,9] on cylinders, is developed to determine the eccentricity between the mass center and geometric center of source masses.

## II. APPARATUS AND PRINCIPLE

The apparatus is shown in Fig. 1. The main component of the device is an aluminum base with a hemispherical groove in the middle. The diameter of the groove is the same as that of the source masses. Compressed air is delivered to a tiny hole at the bottom of the groove. The air is dried and cleaned to minimize its viscous force. The pressure is adjusted to 1–2 times atmospheric pressure by a reducing valve. After careful grinding and polishing, the groove has a nonsphericity of less than 1  $\mu\text{m}$ , and the thickness of the air film is designed to be about 100  $\mu\text{m}$ , so as to minimize the influence of the surface roughness on local pressure. The aluminum mold is placed on three spiral micrometers that can be raised and lowered to adjust the horizontal to less than 2 mrad. Then with the support of high-pressure gas the sphere within the groove will rise and float freely.

If the mass center and geometric center are not coincident, the suspension force  $N$  acting on the geometric center  $O_c$  and the weight  $mg$  acting on mass center  $O_m$  will result in a restoring torque. In this case, the sphere with mass center offset  $e$  will behave as a simple pendulum around point  $O_c$ . The motion equation can be written as

$$I\ddot{\theta} + \gamma\dot{\theta} + mge \sin \theta = \tau, \quad (1)$$

where  $I$  represents the inertia moment of the sphere,  $\gamma$  is the damping coefficient, and  $\tau$  is the external torque that may be introduced by air flow, residual magnetism of the sphere, external disturbance, etc., and is analyzed and discussed in the next section. While the damping is weak and the gravity moment dominates the motion of the sphere, the period of the pendulum can be expressed as

$$T = 2\pi \sqrt{\frac{I}{mge}} K(\theta_0), \quad (2)$$

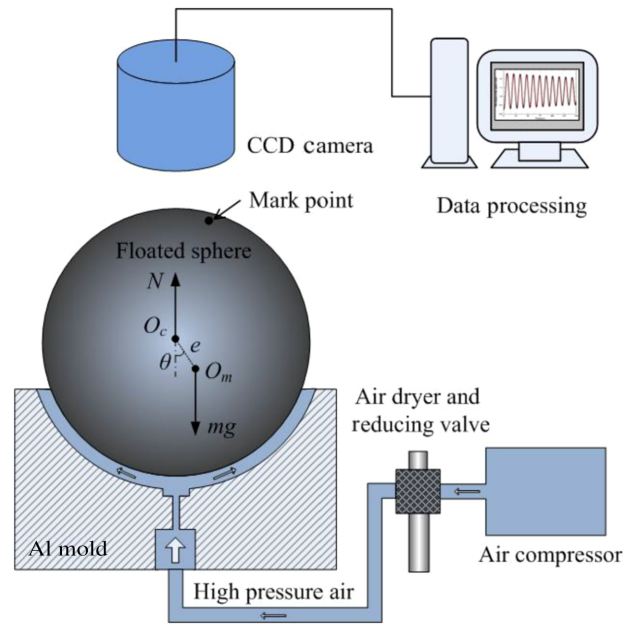


FIG. 1. Apparatus for determining the eccentricity. The sphere is floated by high-pressure air. The suspension force  $N$  acts on geometric center  $O_c$  and the weight  $mg$  acts on mass center  $O_m$ . The sphere will behave as a pendulum. The motion of the sphere is monitored and recorded by a CCD camera. Data processing gives the oscillation period of the sphere and eccentricity  $e$  is obtained from Eq. (4).

where

$$K(\theta_0) = \frac{1}{\sqrt{2\pi}} \int_{-\theta_0}^{\theta_0} \frac{d\theta}{\sqrt{\cos \theta - \cos \theta_0}} \quad (3)$$

is a correction coefficient, which is determined by the amplitude of oscillation  $\theta_0$ . Then the eccentricity can be determined as

$$e = \frac{4\pi^2 I}{mgT^2} K^2(\theta_0). \quad (4)$$

The motion of the floated sphere is monitored and recorded by a CCD camera. For the purpose of observation, on the surface of sphere a small mark point is drawn, the mass of which is negligible for changing the eccentricity. The CCD camera records images of the swing mark in real time at a speed of 28 frames per second, and its coordinates can be obtained by computer image processing. Then fitting the measured data gives the oscillation period of the sphere. And the eccentricity  $e$  can be obtained from Eq. (4).

However, because the sphere can rotate about any axis, it is sensitive to outside disturbance torque, which will make the motion of the sphere too complicated. As a result, a small needle is pressed on the surface of the sphere sideways to limit the motion of the sphere, as shown in Fig. 2. The strength of the force is adjusted just so to make

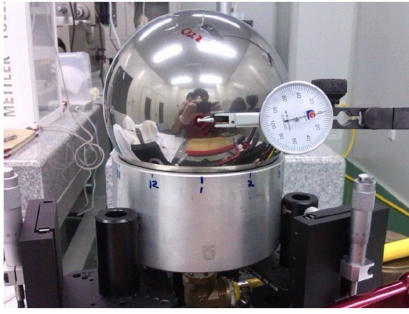


FIG. 2. Photo of the apparatus for the air bearing. A needle with pressure sensor is mounted on the side of the sphere to limit its movement.

the sphere able to rotate around one axis as well as not introducing large damping. In this case, only the eccentricity in one direction can be measured at a time. And to give the total eccentricity  $e$ , three measurements with orthogonal axes  $e_x, e_y, e_z$  are needed:

$$e = \sqrt{\frac{e_x^2 + e_y^2 + e_z^2}{2}}. \quad (5)$$

With the device working, a typical image captured by the CCD camera is shown in Fig. 3(a). The black dot on the sphere in the photo is the mark point, and the pink box around it indicates the position coordinate obtained by image recognition processing. By connecting the coordinates of the mark point in each frame of the video, we get the continuous motion curve of the rotation as shown in Fig. 3(b), then fit it to give the period of the swing motion, and according to Eq. (4) obtain the eccentricity of the sphere.

### III. MEASUREMENT ERROR ANALYSIS

#### A. Uncertainty introduced by direct measurement quantities

Error evaluation is essential in all precision measurement experiments. The uncertainties in the determination

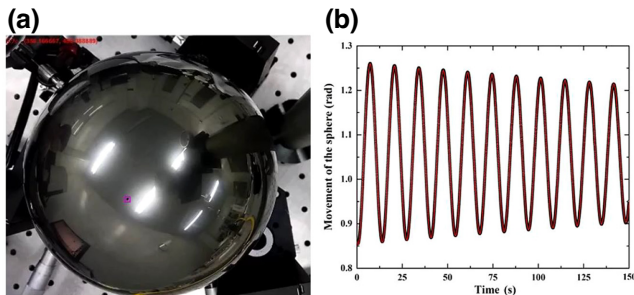


FIG. 3. Image captured by the CCD camera (a) and an obtained continuous motion curve of the swing motion (b).

of eccentricity by the air bearing mainly include two types. One is the uncertainties of each measurement quantity in the experiment, such as the period, swing amplitude, radius of sphere, tilt, air pressure fluctuation, and so on. Since these quantities can be directly measured, this type of error can be evaluated through the respective error transfer formula. For example, one of the improvements of this device is that a CCD camera is used to observe and record the motion of the sphere, so that the period of swing can be extracted by fitting the motion curve with a high accuracy of 0.05 s, which contributes less than 0.01  $\mu\text{m}$  to the uncertainty of the eccentricity measurement. Other main influencing factors are also controlled and the typical values are shown in Table I. The uncertainty contributed by these quantities is within 0.1  $\mu\text{m}$ .

The maximum period that the device can measure is about 120 and 90 s for the 127- and 57-mm spheres, respectively. In the case of a longer period, the motion of the sphere will become irregular, because the restoring moment of the swing, namely the gravity moment introduced by eccentricity, is reduced to the level equivalent to the disturbance torque. In this case, we take the eccentricity corresponding to the maximum period as the measurable minimum eccentricity of the device. In this way, the minimum measurable eccentricity of the device for measuring 127- and 57-mm spheres is 0.56 and 0.20  $\mu\text{m}$ , respectively.

#### B. Uncertainty introduced by disturbance torques

The other major source of uncertainty is the external disturbance torques in the experiment. As it is almost impossible to distinguish the torque exerted by the bearing from the gravitational torque in experiments, both of which vary with the orientation of the sphere, in the experiment we do not attempt to separate the bearing torque from the gravitational torque. We treat the effect that it brings as a measurement uncertainty. How much uncertainty is introduced into the measurement of eccentricity by the torque exerted by the air bearing is estimated.

For a spherical surface element, the forces acting on it by the air bearing mainly include fluid viscosity and fluid pressure. The viscous force is induced by the relative motion of the sphere and airflow, which results in a shear torque always against the rotation of the sphere. Through analysis it can be derived to be of the form  $M_s = -\gamma\dot{\theta}$ , where  $\gamma$  is the damping coefficient, which is mainly determined by the viscosity coefficient of the gas, the thickness of the gas film, and the contact area. In the experiment,  $\gamma$  is obtained to be about  $8 \times 10^{-6}$  N m s/rad by observing the ringdown of the sphere oscillation. The period of this weakly damped system is slightly prolonged and its contribution to the measurement of eccentricity is about 0.01  $\mu\text{m}$ .

Due to the fact that the tested sphere is not an ideal sphere, the direction of the supporting force exerted by the

TABLE I. The main error budget of determining the eccentricity. (Taking a 57-mm-diameter sphere with nonsphericity of 0.27  $\mu\text{m}$  as an example,  $\delta e$  is the respective  $1\sigma$  uncertainty in the eccentricity.)

Parameter	Value	Uncertainty	$\delta e$ ( $\mu\text{m}$ )
Period (s)	>90	0.1	0.01
Swing amplitude (rad)	0.17–0.35	0.1	0.02
Radius of the sphere ( $\mu\text{m}$ )	57 151.87	0.31	0.01
Tilt of the apparatus (mrad)	0	<2	0.01
Orthogonality of three axes (rad)	$\pi/2$	0.1	0.01
Temperature variation ( $^{\circ}\text{C}$ )	22.3	<1.0	0.01
Damping (N m s/rad)	approx. $8 \times 10^{-6}$	$1 \times 10^{-6}$	0.01
Nonsphericity of the sphere ( $\mu\text{m}$ )	0.27	0.09	0.25
Eccentricity	< 0.20		0.25

gas film may not pass through the center of the sphere. As a result, the sphere will be subjected to a torque that drives it to rotate. The disturbance torque generated by the supporting force can be estimated as

$$\vec{M} = \oint P(\vec{r}) \cdot (-\vec{r} \times \vec{n}) dS, \quad (6)$$

where  $P(\vec{r})$  is the pressure distribution that is given clearly according to hydrodynamics,  $\vec{r}$  is the displacement vector from the geometric center  $O_c$  to the surface of sphere, and  $\vec{n}$  is the surface normal unit vector. If the sphere is perfectly spherical,  $\vec{r} \times \vec{n} = 0$ . But for a real sphere, affected by machining accuracy, it is usually not zero.

Take a 57-mm-diameter sphere used in the time-of-swing method as an example. The nonsphericity of the sphere is about 0.22–0.27  $\mu\text{m}$ , measured by a commercial roundness measuring instrument. The instrument can scan only one contour line of a cross section passing through the center of the sphere. We usually scan dozens of the outer contours of the sphere with different orientations. Then according to the maximum estimation of error, the data with the largest nonsphericity are selected to construct the calculation model, for simplicity, assuming the deformations have axial symmetry with a shape given by

$$r = r_0 + \sum a_k \cos k\theta_l, \quad (7)$$

where  $r$  represents the radius and  $\theta_l$  is the orientation of the sphere. The coefficients  $a_k$  are given by the harmonic analysis of the roundness measuring instrument. Shapes with different  $k$  are shown in Fig. 4. This means that the outline of a sphere can be regarded as a superposition of perfect circle, ellipse, and other high-order shapes. A group of typical component coefficients are  $a_2 = 0.082 \mu\text{m}$ ,  $a_3 = 0.012 \mu\text{m}$ ,  $a_4 = 0.009 \mu\text{m}$ ,  $a_5 = 0.012 \mu\text{m}$ , ...,  $a_{50} = 0.004 \mu\text{m}$ , among which  $a_2$  being dominant means an ellipse is the main component of nonsphericity.

Based on the shape of the sphere measured by the roundness measuring instrument, the disturbance torque  $M$  introduced by the nonsphericity is calculated numerically according to Eq. (6), which is a complex integral

over the entire surface of the sphere. The results considering the first 50 harmonics ( $a_2$ – $a_{50}$ ), the first five harmonics ( $a_2$ – $a_5$ ), and the second harmonic ( $a_2$ ) are shown in Fig. 5. The disturbance torques obtained by the sphere model composed of the superposition of harmonics are very close and are in the form of  $M = M_0 \sin 2\theta$ , as  $a_2$  is the dominant component. The sphere will also swing periodically under the action of this moment, which results in a systematic error in the measurement of eccentricity  $\delta e = 2M_0/mg$ . Taking maximum estimation  $M_0 \approx 9.5 \times 10^{-7}$  N m, this corresponds to  $\delta e \approx 0.25 \mu\text{m}$ .

In order to evaluate the influence of the residual magnetism of the sphere on the eccentricity measurement, a magnetic meter with a resolution of 1 nT is used to measure the magnetic field distribution around the spheres, and the measured magnetic moments of the 57- and 127-mm-diameter spheres are less than  $9.8 \times 10^{-8}$  and  $1.3 \times 10^{-3}$  A m<sup>2</sup>, respectively. The moments generated by their interaction with the geomagnetic field are of the order of  $10^{-12}$  and  $10^{-8}$  N m according to the maximum estimation, which are more than 2 orders of magnitude lower than the gravity moment. As a result, the influence of the residual magnetism of the sphere on eccentricity measurement is negligible.

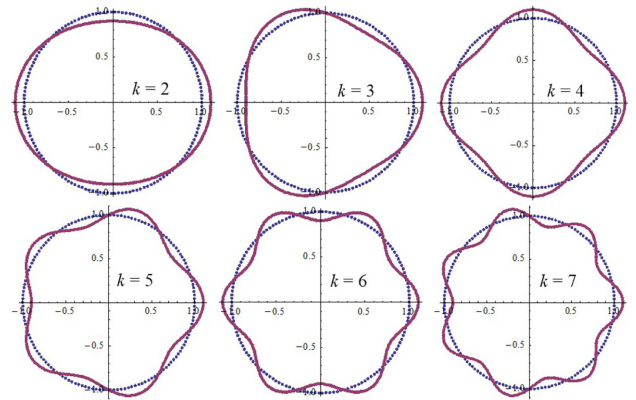


FIG. 4. Shapes described by Eq. (7) with different  $k$ . The outline of a sphere is regarded as a superposition of these shapes.

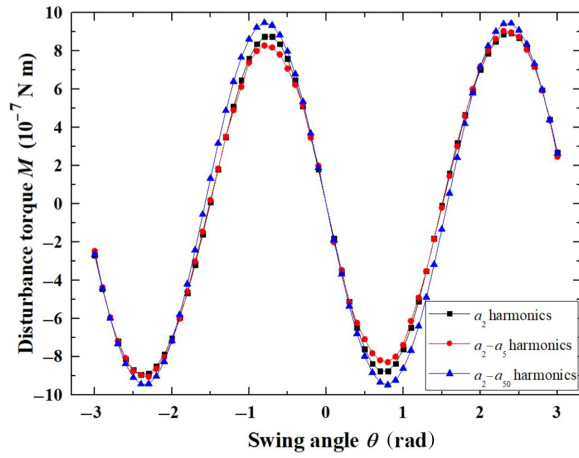


FIG. 5. The disturbance torque  $M$  introduced by the nonsphericity when the sphere is at different swing angle  $\theta$ . The three curves in the figure represent the results considering the first 50 harmonics ( $a_2$ – $a_{50}$ ), the first five harmonics ( $a_2$ – $a_5$ ), and the second harmonic ( $a_2$ ).

A summary of the main error sources in the experiment is presented in Table I. It is clear that the nonsphericity of the sphere is the dominant factor limiting the accuracy of measurement. With this method, the eccentricity introduced by density inhomogeneity of a perfect sphere can be measured to better than  $0.1 \mu\text{m}$ .

An additional experiment is performed to test the sensitivity of the device. At first we measure the mass center offset of a sphere when the sphere rotates as a pendulum about one axis. Then we change the mass center offset by adding mass blocks on the surface of the sphere. The added mass is in line with mass center offset and in the opposite direction. Every time a block with a mass of  $0.03 \text{ g}$  is added. The results of measurements are compared with the calculated mass center offset in Fig. 6. The measured and calculated eccentricities are consistent within their uncertainties and the sensitivity of the air-bearing method is verified to be better than  $0.2 \mu\text{m}$ . With an increase of added mass, the deviation between the measured and calculated eccentricity increases slightly, which is most likely caused by the accumulation of position error of the added masses.

#### IV. RESULTS AND DISCUSSION

The eccentricities of source masses used in our determination of the Newtonian gravitational constant are measured with the air-bearing method. Most of the spheres have a good density uniformity and the eccentricities are less than the detectable minimum of this device. In other words, the swing caused by eccentricity is buried in the disturbance torque caused by nonsphericity. In this case, an upper limit of the eccentricity is given according to the error analysis in Sec. III. The measured results of the source masses are shown in Table II. It shows that the

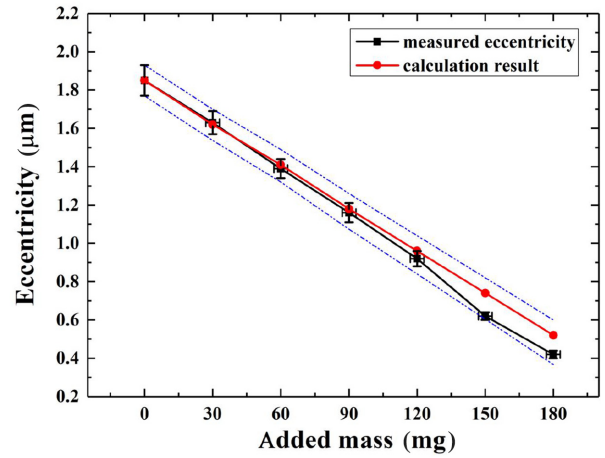


FIG. 6. A comparison of measured results and calculated eccentricity according to added masses. The red points are calculated according to the change of mass center. The black points are measured results using the device.

eccentricity of the 57-mm-diameter spheres used in the time-of-swing method is less than  $0.3 \mu\text{m}$  and that of the 127-mm-diameter spheres used in the angular acceleration feedback method is less than  $1.3 \mu\text{m}$ . Only one sphere shows an obvious periodic oscillation and the measured periods of six random groups of axes are shown in Table III. The results of measurement show good repeatability and are independent of the selection of the three orthogonal axes.

The measured eccentricities are mainly caused by nonsphericities, which in the uncertainty evaluation of  $G$  values are considered in the determination of the geometric center distance between the source masses [11]. Furthermore, we repeat the  $G$  measurements with the orientations of the spheres changed randomly before each run several

TABLE II. The measured eccentricities of source masses used in the  $G$  measurement. Column 3 shows the nonsphericity measured by the roundness measuring instrument. Column 4 shows the measured eccentricity and the evaluated uncertainty (given in parentheses). The uncertainty mainly comes from the influence of disturbance torques by the air bearing, which is highly related to the nonsphericity of the sphere. Spheres 1–4 are used in the TOS method and spheres 9–12 are used in the AAF method.

No.	Diameter (mm)	Nonsphericity ( $\mu\text{m}$ )	Eccentricity ( $\mu\text{m}$ )
1	57.15072(25)	0.22(3)	<0.20(21)
2	57.15236(30)	0.23(3)	<0.20(22)
3	57.14577(25)	0.23(3)	<0.20(22)
4	57.15187(31)	0.27(9)	<0.20(25)
9	127.0003(8)	0.75(6)	<0.56(73)
10	126.9957(9)	0.75(6)	<0.56(73)
11	126.9934(8)	0.72(6)	<0.56(70)
12	126.9887(10)	0.89(11)	1.25(86)

TABLE III. The measured swing periods  $T$  and eccentricity  $e$  of sphere 12 used in the AAF method about six random groups of axes.

$i$	$T_{x_i \text{ axis}} \text{ (s)}$	$T_{y_i \text{ axis}} \text{ (s)}$	$T_{z_i \text{ axis}} \text{ (s)}$	$e_i \text{ (}\mu\text{m)}$	Average $\bar{e} \text{ (}\mu\text{m)}$
1	81.7(2)	117.3(2)	69.9(2)	1.24(86)	1.25(86)
2	86.8(1)	69.3(1)	106.5(2)	1.23(86)	
3	72.5(2)	99.9(3)	71.8(1)	1.36(86)	
4	84.1(3)	83.8(1)	77.6(1)	1.22(86)	
5	95.3(2)	85.1(2)	68.9(1)	1.29(86)	
6	67.3(1)	113.4(4)	120.0(1)	1.15(86)	

times. The statistical error evaluation of measured  $G$  values includes the influence of sphere density uniformity and sphere nonsphericity.

Since a small eccentricity of 1.25(86)  $\mu\text{m}$  is found in sphere 12 used in the  $G$  measurement by the AAF method, we especially analyze the uncertainty it may introduce. To estimate the uncertainty in  $G$  value resulting from the eccentricities of source masses, we propose two models of density distribution with eccentricities equal to the results measured. In the first model, we suppose that the eccentricities of the attracting spheres are due to air bubbles in the spheres, and take the maximum estimation whereby we assume that there is only one spherical bubble in each sphere. We assume that the distribution probability of sphere eccentricity in all directions is equal. Then the average uncertainty contribution of eccentricity equals the influence on determining  $G$  of each sphere in one direction times the probability of the sphere eccentricity in this direction. The data processing is similar to that of Refs. [12,13]. An average uncertainty of 4.01 ppm in the AAF method is introduced by the eccentricity.

In the second model, we suppose that the density of each sphere has a linear distribution. The distribution of a sphere's density along the  $x$  axis can be expressed as  $\rho = \rho_0(1 + kx)$ . According to  $e = \int (x\rho)dV / \int \rho dV$ , the value of  $k$  causes the eccentricity and can be calculated as  $k = 5e/R^2$ , where  $R$  is the radius of the sphere. When the  $x$  axis is the direction of the sphere scaling with pendulum, the uncertainty in  $G$  by density uniformity reaches its maximum. Similarly we suppose the eccentricity in all directions has the same probability. The effect is calculated with the sphere at all orientations, and then multiplying by the probability of the sphere lying at this orientation gives the evaluation of the uncertainty contribution of the eccentricity, which is 3.84 ppm in the AAF method.

The above analysis gives the error contribution to the  $G$  measurement that may be introduced by two extreme cases. The measured data show that the actual situation is a little more optimistic than the above results. In the experiment with the AAF method, to average out the density inhomogeneity effect of the source masses, 29 sets of data are recorded with the orientation of each sphere

changed by a random azimuthal angle. The statistical error of angular acceleration  $\alpha_r$  is determined to be less than 3.44 ppm [11], within which the uncertainty contributed by the density inhomogeneity of spheres is included.

## V. CONCLUSION

In summary, we present an air-bearing method to measure the mass center offset from the geometric center of spheres in determining  $G$ . By introducing a CCD camera for observation and image processing to obtain the data, the measurement accuracy of this method is greatly improved. The uncertainty of eccentricity is analyzed in detail and is mainly limited by the nonsphericities of the spheres. Density distribution models in two extreme cases are discussed to estimate the uncertainty in the value of  $G$  caused by the eccentricities of source masses and the result shows that a maximum uncertainty of several ppm may be introduced. By changing the orientations of source masses, repeated measurements can further effectively average out the effects of density inhomogeneity and nonsphericity.

## ACKNOWLEDGMENTS

The authors thank Dr. L. Zhu for useful discussions, and we are grateful to Mr. Xiong for his hard work in grinding spheres and the groove. This work is supported by the National Natural Science Foundation of China under Grants No. 12105373 and No. 11975319, the Guangdong Basic and Applied Basic Research Foundation under Grant No. 2019A1515110697, and the China Postdoctoral Science Foundation under Grant No. 2019M663228.

- 
- [1] G. T. Gillies and C. S. Unnikrishnan, The attracting masses in measurements of  $G$ : An overview of physical characteristics and performance, *Phil. Trans. R. Soc. A* **372**, 20140022 (2014).
  - [2] R. Newman, M. Bantel, E. Berg, and W. Cross, A measurement of  $G$  with a cryogenic torsion pendulum, *Phil. Trans. R. Soc. A* **372**, 20140025 (2014).
  - [3] J. H. Gundlach and S. M. Merkowitz, Measurement of Newton's Constant Using a Torsion Balance with Angular Acceleration feedback, *Phys. Rev. Lett.* **85**, 2869 (2000).
  - [4] T. R. Armstrong and M. P. Fitzgerald, New Measurements of  $G$  Using the Measurement Standards Laboratory Torsion Balance, *Phys. Rev. Lett.* **91**, 201101 (2003).
  - [5] St. Schlamminger, E. Holzschuh, W. Kündig, F. Nolting, R. E. Pixley, J. Schurr, and U. Straumann, Measurement of Newton's gravitational constant, *Phys. Rev. D* **74**, 082001 (2006).
  - [6] G. Rosi, F. Sorrentino, L. Cacciapuoti, M. Prevedelli, and G. M. Tino, Precision measurement of the Newtonian gravitational constant using cold atoms, *Nature* **510**, 518 (2014).

- [7] H. V. Parks and J. E. Faller, Simple Pendulum Determination of the Gravitational Constant, *Phys. Rev. Lett.* **105**, 110801 (2010).
- [8] T. J. Quinn, C. C. Speake, S. J. Richman, R. S. Davis, and A. Picard, A New Determination of  $G$  Using Two Methods, *Phys. Rev. Lett.* **87**, 111101 (2001).
- [9] T. J. Quinn, H. V. Parks, C. C. Speake, and R. S. Davis, Improved Determination of  $G$  Using Two Methods, *Phys. Rev. Lett.* **111**, 101102 (2013).
- [10] P. J. Mohr, D. B. Newell, and B. N. Taylor, CODATA recommended values of the fundamental physical constants: 2014, *Rev. Mod. Phys.* **84**, 035009 (2016).
- [11] Q. L. i. C. Xue, J. P. Liu, J. F. Wu, S. Q. Yang, C. G. Shao, L. D. Quan, W. H. Tan, L. C. Tu, and Q. Liu, *et al.*, Measurements of the gravitational constant using two independent methods, *Nature* **560**, 582 (2018).
- [12] L. X. Liu, C. G. Shao, L. C. Tu, and J. Luo, Measurement of density inhomogeneity for source masses in time-of-swing method of measuring  $G$ , *Chin. Phys. Lett.* **26**, 010403 (2009).
- [13] J. Q. Guo, Z. K. Hu, B. M. Gu, and J. Luo, Measurement of eccentricity of the centre of mass from the geometric centre of a sphere, *Chin. Phys. Lett.* **21**, 612 (2004).